ISSN 0023-1584, Kinetics and Catalysis, 2006, Vol. 47, No. 1, pp. 25–34. © MAIK "Nauka/Interperiodica" (Russia), 2006.
Original Russian Text © M.V. Tsodikov, V.V. Teplyakov, M.I. Magsumov, E.I. Shkol'nikov, E.V. Sidorova, V.V. Volkov, F. Kapteijn, L. Gora, L.I. Trusov, V.I. Uvarov, 2006, published in Kinetika i Kataliz, 2006, Vol. 47, No. 1, pp. 29–39.

HIGHLY ORGANIZED CATALYTIC SYSTEMS

Ceramic Membranes Modified with Catalytic Oxide Films as Ensembles of Catalytic Nanoreactors

M. V. Tsodikov*, V. V. Teplyakov*, M. I. Magsumov*, E. I. Shkol'nikov*, E. V. Sidorova*, V. V. Volkov*, F. Kapteijn, L. Gora**, L. I. Trusov***, and V. I. Uvarov******

** Topchiev Institute of Petrochemical Synthesis, Russian Academy of Sciences, Moscow, 117912 Russia*

*** Delft University, the Netherlands*

**** Aspekt Research and Production Association, Obninsk, Kaluga oblast, Russia*

***** Institute of Structural Macrokinetics, Russian Academy of Sciences, Chernogolovka, Moscow oblast, 142432 Russia*

Received October 27, 2004

Abstract—Hybrid catalytic membrane systems have been produced by modifying porous ceramic membranes with metal oxide films. A two-layer cermet membrane consisting of a flexible stainless steel layer and an overlying porous TiO_2 ceramic layer and a ceramic titanium carbide membrane are examined. The membrane surfaces have been modified by the alkoxide method using colloidal organic solutions of metal complex precursors. Producing a tetragonal single-phase ZrO_2/Y_2O_3 coating on the cermet surface increases the abrasion strength of the ceramic layer. CO oxidation and the oxidative conversion of methane into synthesis gas and light hydrocarbons can be markedly intensified by modifying the membrane channels with $Cu_{0.03}Ti_{0.97}O_{2\pm\delta}$ and La + Ce/MgO catalysts, respectively. A method has been developed for depositing, onto the geometrical surface of a membrane, a film of the new single-phase oxide $P_{0.03}Ti_{0.97}O_{2\pm\delta}$ with an anatase structure and uniform pores of mean diameter $\langle d \rangle \sim 2$ nm. Blocks of zeolite-like silicalite can be formed on the surface of the phosphorus–titanium oxide film. The resulting hybrid membrane is characterized by an anisotropic permeability depending on the flow direction. This property has an effect on conversion and selectivity in the nonoxidative dehydrogenation of methanol.

DOI: 10.1134/S0023158406010058

In recent years, much attention has been focused on heterogeneous catalytic reactions using porous membranes [1–3]. Research in this field has been stimulated by the challenging problems of raising the selectivity of reactions without significantly impairing their efficiency and of reducing their energy intensity. Note that this research has received an impetus from the development of a new generation of membrane materials [4, 5]. Membranes have customarily been used to reduce the energy intensity of the pretreatment of raw materials and to selectively separate the desired products [4, 5]. A new line of research in this area is the development of a microreactor that can combine a high rate of catalytic conversion with selective product transport. Such a microreactor can be membrane channels modified with finely dispersed catalysts. In the general case, gas transport in porous media is due to viscous, slip, surface, or molecular flow [6, 7]. Catalytic films with a large specific surface area imply a large ratio of the surface area of the film to the volume of the transport pores (S/V). It can, therefore, be expected that the frequency of the interaction between molecules and pore walls will be high and that catalytic reactions will proceed more rapidly in such systems than in macroreactors.

A promising way of producing catalytic oxide films in the channels of ceramic membranes is by using alkoxide methods, which allow catalytic oxide systems to be prepared from sols of metal complex precursors [8, 9].

Here, we report a directional method for the modification of ceramic membranes in order to obtain hybrid membrane and catalytic membrane systems and present data characterizing the catalytic activity of these systems in reactions involving C_1 compounds.

EXPERIMENTAL

We used two types of microporous membrane, namely, a Trumem™ cermet membrane and a BUM ceramic membrane as tubes (diameter, 14 mm; length, 20 cm; geometrical surface area, 82 cm^2) and discs (diameter, 40 mm; thickness, 3 mm; geometrical surface area, 8 cm^2) [10, 11]. The cermet membrane has a two-layer composite structure consisting of an SS316L porous stainless steel substrate (thickness, 200 μm; mean pore size, 2 μm; specific surface area, $\sim 1.5 \times 10^4$ cm^2/cm^3) and an overlying rutile ceramic layer (thickness, 20 μm; mean pore size, 0.13 μm; specific

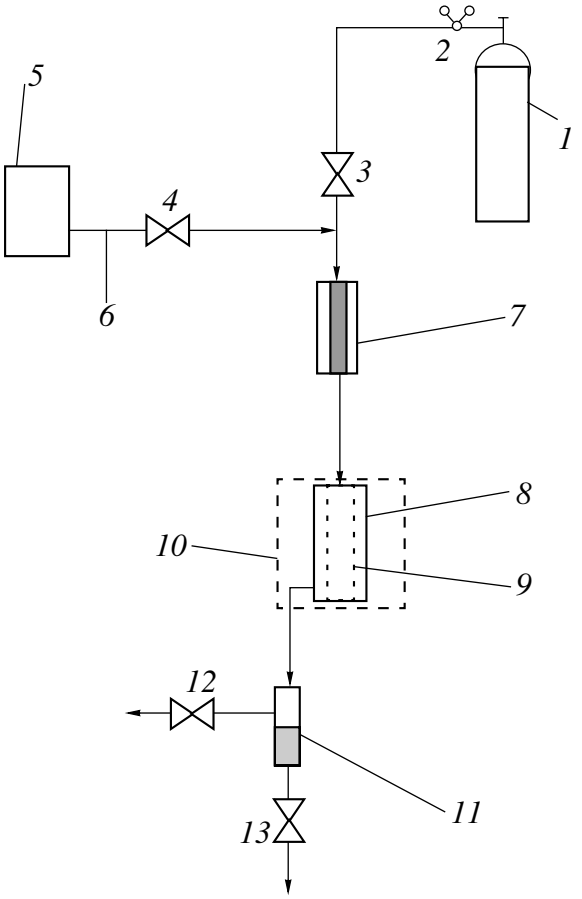

Fig. 1. Schematic of the laboratory setup for testing catalytic tubular membranes: (*1*) gas cylinder, (*2*) pressure regulator, (*3*, *4*, *12*, *13*) valves, (*5*) doser, (*6*) liquid pipeline, (*7*) preheating furnace (evaporator), (*8*) reactor, (*9*) membrane, (*10*) reactor furnace, and (*11*) separator.

surface area, ~2×10^5 cm^2/cm^3; porosity, 30–35%; air permeability, 330–400 m$^3 \times 10^3$ l h^{-1} m^{-2} atm^{-1}).

The BUM ceramic membrane is based on titanium carbide and has a mean pore size of ~5 μm, a porosity of ~60%, a wall thickness of 3 mm, and an air permeability of 1500 m^3/(m^2 h atm). Specific features of the ceramic membrane are that it shows a high thermal stability and can be regenerated by heat treatment or by acid washing.

Catalytic metal oxide layers inside membrane channels were formed by an alkoxide method. Oxides of desired composition were obtained from toluene solutions containing appropriate amounts of metal complex precursors and solution stabilizers [12]. In order to modify the internal membrane surface, a mother solution of a metal complex precursor was pumped through the membrane using a laboratory setup attached to a vacuum pump. Next, the membrane was blown with humidified hot air, dried *in vacuo* (1 Torr), and heated in various regimes.

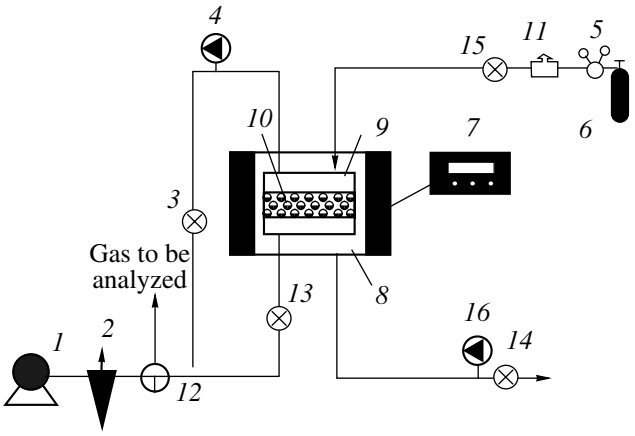

Fig. 2. Schematic of the laboratory setup for testing catalytic disc-shaped membranes in the temperature range 20–1200°C: (*1*) vacuum pump, (*2*) cold trap, (*3*, *13–15*) gas valves, (*4*, *16*) pressure–vacuum gages, (*5*) pressure regulator, (*6*) gas cylinder, (*7*) temperature control, (*8*) diffusion cell furnace, (*9*) diffusion cell, (*10*) membrane, (*11*) metering valve, and (*12*) three-way valve.

Oxide films were obtained on the geometrical surface of the membrane by the spin coating method [13]. A mother solution was fed onto the surface of a spinning membrane at a rate of 2–3 drops per second. The rotational speed of the membrane was 1800–2000 rpm. The solution was dropped while blowing the membrane with humid air. Thereafter, the membrane was heat-treated in various regimes. The amount of oxide introduced was determined gravimetrically.

In order to increase the mechanical strength of the cermet membrane, the inner surface of the disc was coated with a thin layer of ZrO_2 modified with 5 mol % Y_2O_3, with a tetragonal structure, which is known to be mechanically very strong [14]. For this purpose, we used a mother solution containing solvated zirconium isopropoxide ($Zr(OPr^i)_4$ Pr^iOH) and yttrium acetylacetonate ($Y(acac)_3$). The preparation of this solution is described elsewhere [15, 16]. Next, the membrane was dried, heat-treated in Ar at 300°C, and calcined in a muffle furnace at 900°C and $P = 10^{-3}$ Torr for 6 h.

The abrasion resistance of membranes was determined using a laboratory setup designed by NPO Aspekt (Obninsk) [10]. The disc-shaped membrane to be tested, secured in a rotating chuck, was abraded for 1 h. Abrasion resistance was evaluated in terms of the relative weight lost by the ceramic layer upon 1-h-long abrasion.

The catalytic activity of the modified tubular and disc-shaped membranes was measured in two types of flow reactor fitted with precision pressure gages, a chromel–alumel thermocouple for measuring the reaction zone temperature, and automated temperature regulators [12].

Figure 1 schematizes the setup used in the testing of tubular catalytic membranes. The Trumem^{TM} cermet

membrane was soldered with a silver solder to the inlet and outlet pipes of the reactor. The ceramic membrane tube was secured in the reactor using high-temperature sealing materials.

For the disc-shaped membranes, we used the flow setup shown in Fig. 2. These membranes were tested in a special-purpose diffusion cell, which could also be used in gas permeability measurements.

For CO oxidation, $Cu_{0.03}Ti_{0.97}O_2$ oxide systems with an anatase structure and $0.05NiO \cdot 0.95Al_2O_3$ systems with a spinel structure, which proved to be catalytically active in this reaction, were produced inside membrane channels. The preparation of these systems is detailed elsewhere [12].

In CO oxidation tests, which were carried out in the transmembrane transfer mode, the initial gas mixture at a gage pressure of 0.11–0.15 MPa was filtered through a tubular or disc-shaped membrane.

CO and O_2 concentrations in the initial gas mixture and in the reaction product were determined in the on-line mode using a Riken Keiki gas analyzer with an IR spectroscopic cell and a Beckman gas analyzer with an electrochemical cell.

Gas mixtures containing various CO and O_2 concentrations, diluted with special-purity nitrogen, were fed to the inner side of the membrane.

The CO oxidation rate was determined as in the case of a plug-flow reactor:

$$r = \frac{dX_i}{d\tau_i}, \quad (1)$$

where X_i is conversion (in mole fractions); τ_i is the physical contact time per mole of the reactant:

$$\tau_i = \frac{S \times 22400 \times 100}{WC_{i,0} \times 60}, \quad \frac{\text{cm}^2\ \text{h}}{\text{mol}_{\text{CO}}}. \quad (2)$$

Here, C_i is the volumetric concentration of the ith reactant (CO or O_2) in the initial gas mixture (% vol), S is the geometrical surface area of the membrane (cm^2), and W is the volumetric gas flow rate (cm^3(STP)/min). The calculation of macrokinetic parameters is described elsewhere [12].

Methane oxidation was studied on the BUM ceramic tubular membrane.

This membrane was coated with catalysts using a two-step procedure. In the first step, a rutile buffer film was formed on the membrane by successively depositing five titanium dioxide layers from a 10% titanium tetrabutoxide solution in toluene. After the deposition of each two layers, the membrane was dried and calcined at 500–600°C. In the second step, we formed two catalytic coatings simulating the (La + Ce)/MgO and cubic ZrO_2/Y_2O_3 catalysts.

In the preparation of the cerium–lanthanum system, we used a nitric acid solution of La and Ce and a toluene solution of magnesium acetylacetonate. Initially, ten magnesium acetylacetonate layers were deposited from the toluene solution onto the titanium dioxide buffer film and the product was dried and calcined at 500°C. Next, lanthanum and cerium oxides were produced on the magnesium oxide surface to the extent of 5% relative to the MgO. The lanthanum–cerium mixture was deposited from a methanolic solution of acetylacetonate complexes. Cubic ZrO_2/Y_2O_3 was deposited by pumping, through the membrane, a toluene solution of solvated zirconium isopropoxide and yttrium acetylacetonate (9 mol % Y_2O_3 relative to the zirconium dioxide).

Oxidative methane conversion runs were carried out in the transmembrane transfer mode at a pressure of ~1.5 atm in a catalytic flow reactor. The initial gas mixture was fed to the inner side of the membrane. The gaseous methane conversion products on the outer side of the membrane were cooled and analyzed by on-line gas chromatography.

Methanol conversion tests were carried out in the membrane mode using tubular and disc-shaped cermet membranes. For this reaction, a $Cr_2O_3 \cdot Al_2O_3 \cdot ZnO$ catalytic film simulating an earlier reported industrial catalyst [17] was produced inside membrane channels. The zinc–chromium–aluminum system was prepared from zinc and chromium acetylacetonates and a 60% aluminum isobutoxide solution in isobutyl alcohol. The catalytic oxide film was formed under the same conditons as the CO oxidation catalysts (see above).

The tubular and disc-shaped membranes were tested in a flow reactor. The tests were carried out in the membrane mode by transferring the gas reactants through the tubular and disc-shaped catalytic membranes at a gage pressure of 0.13–0.17 MPa. Most of the methanol vapor in Ar diffused in the cell over the catalytic disc-shaped membrane. By changing the pressure drop, part of the gas mixture was forced to diffuse through membrane channels. The liquefiable components of the gas mixture passing through the cell chamber and the membrane channels were condensed and weighed.

The methane and methanol conversion products were analyzed by gas chromatography on an LKhM 80 chromatograph. H_2, CO_2, CO, and CH_4 were determined using a 4×150 mm column packed with SKT carbon, argon as the carrier gas, and a thermal-conductivity detector. The hydrocarbons resulting from the reaction were determined using a 4×200 mm column packed with 5% squalane/α-Al_2O_3, helium as the carrier gas, and a flame-ionization detector.

For the formation of a metal oxide mesoporous membrane, the cermet was coated with a thin layer of the $P_{0.03}Ti_{0.97}O_2$ compound by the spin-coating method. This compound is characterized by a uniform pore size of ~2 nm [18].

A thin phosphorus–titanium oxide film was obtained from $Ti(OBu)_4$ and etriol phosphite [18] by dropping a toluene solution of these compounds (0.25 cm^3) at a rate of 3 drops per second onto a mem-

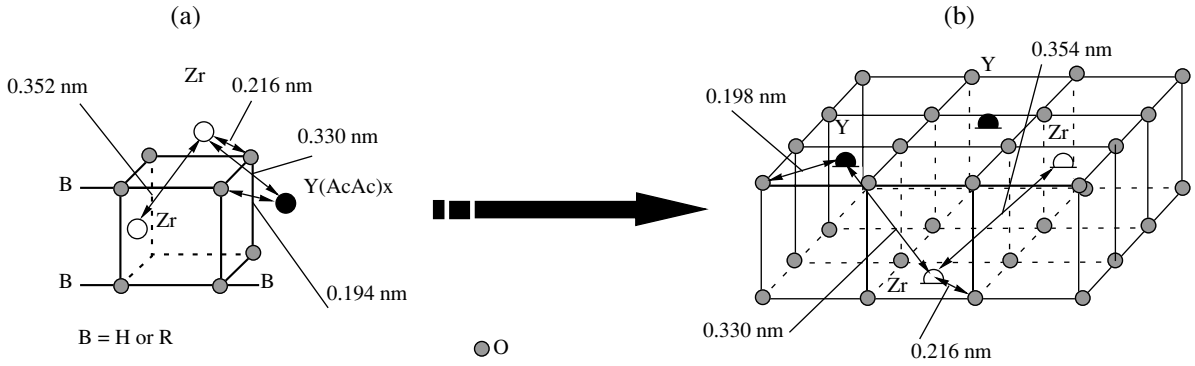

Fig. 3. ZrO_2/Y_2O_3 (a) sol and (b) crystal structures according to EXAFS data [24].

brane rotating with a speed of 2000 rpm while blowing the membrane with humid air. After a gel was formed on the surface of the Trumem disc, the system was heat-treated at 500°C in Ar for a short time. After the fifth layer was thus obtained, the system was heated to 500°C at a rate of 5 K/min in a muffle furnace and was held at this temperature for 6 h.

Oriented silicalite crystals on the $P_{0.03}Ti_{0.97}O_2$ surface were obtained from a mother as described in [19]. The $Na_2O : Al_2O_3 : SiO_2 : H_2O = 41.9 : 1.0 : 4.4 : 833.3$ zeolite was obtained from an aqueous solution containing $NaAlO_2$ and $Na_2SiO_3 \cdot 5H_2O$. This solution, in a capsule, was aged for 1 h at room temperature. The synthesis was carried out at 80°C for 4 h. After the synthesis, the system was immersed in cold water for 5 min. The morphology of the film was studied by scanning electron microscopy with a Phillips XL 30 FEG SEM microscope combined with a Bruker-AXS D 5005 electron-probe X-ray microanalyzer.

Gas permeability was measured using a membrane diffusion cell (Fig. 2) in the vacuum–compression mode. The inlet pressure (P_{in}) was maintained at 1.5–2.5 atm, and the outlet pressure was $P_{out} = 0.2$–0.5 atm. Gas permeability was calculated using the formula

$$Q = J/\Delta PA, \quad (3)$$

where Q is the gas permeability of the membrane (l (STP) h^{-1} m^{-2} atm^{-1}), J is the gas flux through the membrane (l (STP)/h), $\Delta P = P_{in} - P_{out}$ is the pressure drop across the membrane (atm), and A is the membrane surface area (m^2).

The pore structure of the membrane was characterized by dynamic desorption porosimetry [20].

RESULTS AND DISCUSSION

The ceramic layers of the flexible membranes have an insufficient abrasion resistance. In view of this, one of the main tasks at the first stage of our study was to produce a thin and mechanically strong film. As was noted above, yttria-modified zirconium dioxide with a tetragonal structure has a high mechanical strength that depends critically on its phase purity [21, 22].

Earlier, we developed an original method for preparing single-phase tetragonal and cubic zirconia from zirconium isopropoxide and acetylacetonate complexes [15, 16]. It was demonstrated that the complexes interact even in the organic sol to yield a heterometallic precursor of the oxide [23, 24]. In the amorphous gel, there are already local polyhedral oxide structures surrounded by acetylacetonate, alkoxide, and hydroxide ligands (Fig. 3). In the ceramics obtained from the zirconium–yttrium gel, tetragonal ZrO_2/Y_2O_3 nanoclusters are characterized by a narrow size distribution around a mean crystallite size of 4–6 nm [22]. After five layers of the zirconium–yttrium sol were applied to the inner walls of the Trumem tube, the abrasion resistance of the membrane estimated from weight loss data was found to be higher by more than one order of magnitude

Table 1. Abrasion resistance of the cermet membrane modified with a thin ZrO_2/Y_2O_3 film with a tetragonal structure

Description	Pore size, μm		Water permeability, cm^3/cm^2	Abrasion resistance (weight loss), rel. units
	D_{max}	D_{mean}		
Unmodified	1.00	0.16	4000	257
Modified	1.04	0.16	4000	16
Unmodified	1.00	0.11	2400	22
Modified	0.84	0.10	2400	1

(Table 1). As is clear from Table 1, the water permeability of the modified membrane is almost unchanged. As estimated from the Ar permeability of the modified cermet membrane, the thickness of the zirconate does not exceed 25 ± 5 nm.

The catalytic membrane module was used in the measurement of catalytic activity in CO oxidation, in the oxidative dehydrogenation of methane, in the conversion of methanol into synthesis gas, and in nonoxidative dehydrogenation.

A challenging environmental problem is to carry out efficient CO oxidation in lean mixtures, particularly industrial and automobile exhaust gases. Increasing the rate of CO oxidation is also of great importance for the design of a new generation of air conditioners.

Ceramic membranes consisting of titanium carbide and oxide are inactive in CO oxidation. At the same time, carbon monoxide is oxidized at an appreciable rate as the gas mixture is transferred through a membrane whose channels have catalytic oxide films inside. Figure 4 plots the temperature dependences of the extent of CO oxidation for various membranes and catalysts at a fixed relative weight of catalyst introduced. Clearly, the way the CO conversion varies with temperature depends strongly on the nature of the catalyst and on the membrane's channel size. The highest CO conversion is observed for the cermet membrane coated with copper–titanium oxide. It is approximately one order of magnitude higher than the conversion attainable with catalyst pellets of the same composition [25]. Furthermore, CO conversion is much higher on the cermet membrane than on the ceramic membrane, although the ratio of the channel length to the effective channel diameter for the cermet membrane ($l/d \approx 200$) is approximately one order of magnitude smaller than the same ratio for the ceramic membrane ($l/d \approx 1000$). It is likely that the determining factor in CO conversion is pore size, which is one order of magnitude smaller in the cermet membrane than in the ceramic membrane. It is not impossible that the process depends considerably on the pore configuration and tortuosity.

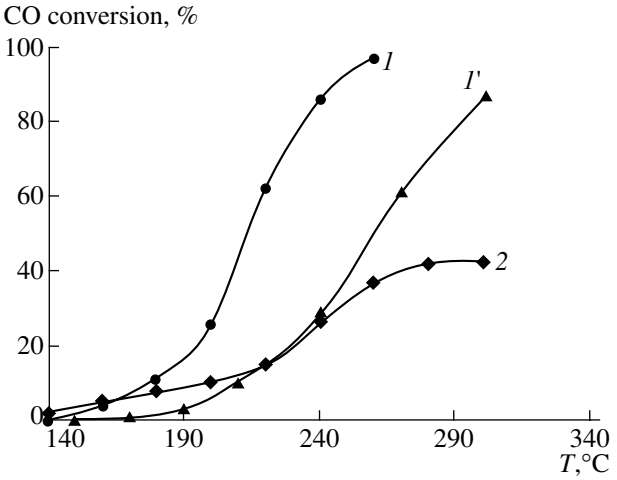

Fig. 4. Extent of CO oxidation as a function of channel diameter and reaction temperature for (*1*, *1'*) cermet and (*2*) ceramic membranes modified with (*1*, *2*) $Cu_{0.03}Ti_{0.985}O_2$ and (*1'*) $NiOAl_2O_3$. The channel sizes in the original membranes are (*1*, *1'*) ⟨0.13⟩ and (*2*) ⟨1⟩ μ.

With the catalytic membrane module containing the copper–titanium oxide catalytic system, a nearly 100% CO conversion is achieved at 250°C at a residence time of 10^{-3} s, which is the time taken by reactant molecules in the reaction zone to diffuse through the membrane wall. Kinetic studies have demonstrated that CO oxidation is satisfactorily described by a first-order rate equation [12]. Increasing the amount of catalytic film inside the membrane channels raises the rate constant.

Table 2 lists data characterizing the permeability and effective cross-sectional area of the membranes and the specific surface area of the catalytic films inside the membrane channels. These data suggest that catalytic

Table 2. Amount of catalyst ($Cu_{0.03}Ti_{0.985}O_2$) deposited, the specific surface area and permeability of the membrane, and the properties of the catalytic film

Type of membrane	Amount of catalyst deposited, g/cm^3	Permeability, 1 (DTP) m^{-2} h^{-1} atm^{-1}	Parameters calculated for a continuous film			Parameters derived from permeability data		Specific surface area of the catalytic film, m^2/g$_{membr}$
			pore size, μm	film thickness, μm	inner surface area, m^2	pore size, μm	film thickness, μm	
BUM	0.225	1142000	4.26	0.10	0.213	3.95	0.25	8.3
	0.380	765400	4.11	0.18	0.195	3.21	0.36	13.3
	0.700	304000	3.79	0.34	0.190	2.16	1.15	25.5
Trumem	0.900	240000	–	–	–	–	–	32.8

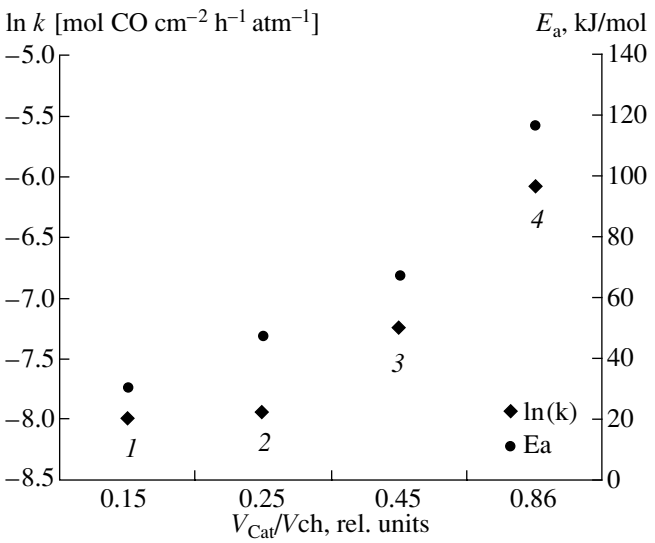

Fig. 5. Logarithm of the rate constant at 220°C and apparent activation energy versus the channel fraction filled with catalyst for the (*1–3*) ceramic and (*4*) cermet membranes.

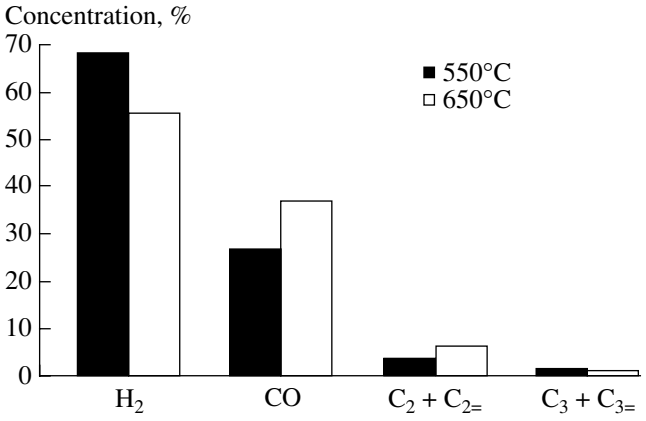

Fig. 6. Product composition diagram for methane oxidation on the La–Ce/MgO catalyst at various temperatures. Methane conversion is 22.5% at 550°C and 33.4% at 650°C.

CO oxidation develops when the gas moves in the nonselective viscous flow regime.

A specific feature of this reaction in the catalytic microchannels is that both of its basic kinetic parameters—effective rate constant and activation energy—increase as the amount of catalyst is increased from 0.22 to 0.90 g/cm^3 and the temperature is elevated from 180 to 220°C, indicating that this reaction is of the compensation type (Fig. 5), which is rather rare in heterogeneous catalysis [26–28].

The increase in the rate constant of oxidation is due to the fact that the preexponential factor increases nearly by nine orders of magnitude. An increasing preexponential factor is usually an indication of a growing number of active sites and, accordingly, an increasing statistical number of active collisions between reacting substrate molecules and the active surface. Further investigation is necessary to understand the reason why increasing the amount of a given catalyst causes an increase in the Arrhenius parameter from 30 to 116 kJ/mol. In an earlier study [12], it was assumed that the active sites are statistically independent and the theorem of the relative fluctuation of an additive state function was applied to a system consisting of N independent parts [29]:

$$\delta = 1/\sqrt{N} \sim 1/\sqrt{k_0},$$

where N is the number of active sites [29, 30].

It can readily be seen that, if the preexponential factor k_0 indirectly reflects the number of excited states (N), then the relative quantity δ (δ_n/δ_1, where n is the number of successive catalyst layers), which characterizes the mean relative fluctuation of energy, will decrease markedly with an increasing amount of catalyst, taking values of 1, 0.123, and 0.002. Therefore, the statistical number of CO molecules whose energy is sufficient to overcome the potential energy barrier of the reaction is likely to decrease with an increasing amount of catalyst in the membrane channels. This is manifested as an increasing activation parameter of the reaction. Increasing the amount of catalyst is believed to cause structural changes in the mixed oxide formed inside the channels. A possible change of this kind is an increase in the size of the microcrystallites containing active sites, which may alter the active surface area. At the same time, this will markedly increase the number (probability) of active collisions. This deduction is confirmed by the increase in the order of magnitude of the preexponential factor, the quantity making the largest contribution to the increase in the oxidation rate constant.

Another reaction that was studied under flow conditions is methane oxidation. The conversion of methane into important petrochemical products is among the priority research fields. It is, therefore, necessary to develop an appropriate class of catalytic systems for this purpose.

Methane oxidation was carried out in the presence of the La–Ce/MgO and La–Ce/ZrO_2–Y_2O_3 catalytic systems with a cubic structure. Earlier, it was demonstrated that methane can be selectively oxidized to C_2 and C_3 olefins at 750–850°C over the La–Ce/MgO system in a flow reactor [31]. At elevated temperatures, cubic zirconia is anion-conducting due to the transport of lattice oxygen. It was, therefore, expected that the lattice oxygen of the surface would be spent for the selective oxidation of methane and that the resulting defects would be "healed" by air oxygen present in the reaction mixture. It was found that extensive coking occurs at a high methane conversion, which is 60% at 550°C and 70% at 650°C in the presence of the zirconate system. The coke yield is as high as 80%, and the remaining 20% is synthesis gas with H_2 : CO = 1 : 1. In

the presence of the La–Ce/MgO system under the same conditions, the synthesis gas selectivity is much higher. Figure 6 shows a diagram illustrating the composition of the reaction products. At methane conversion values of 25 and 35%, the synthesis gas selectivity is 70 and 80%, respectively; the H_2 : CO ratio is approximately 2.5 : 1 and 1.5 : 1, respectively; and the C_2–C_4 hydrocarbon selectivity is up to 5–10%. Regenerating the catalytic system with atmospheric oxygen almost restores the original catalytic activity.

The product composition resulting from partial methane oxidation in the catalytic membrane module differs from the product composition observed for a flow reactor, in which the main reaction products are ethylene and propylene [31]. Note, however, that, as compared to the flow reactor, the catalytic membrane module affords nearly the same conversion at temperatures lower by 100 to 170 K.

The methanol conversion reactions yielding synthesis gas, methane, and formaldehyde are endothermic [32]:

$$1.\ CH_3OH \Rightarrow CO + 2H_2, \quad \Delta Q = 100.3\ \text{kJ/mol}.$$

$$2.\ CH_3OH + H_2 \Rightarrow CH_4 + H_2O, \quad \Delta Q = 117.6\ \text{kJ/mol}.$$

$$3.\ CH_3OH \Rightarrow CH_2O + H_2, \quad \Delta Q = 91, 3\ \text{kJ/mol}.$$

The main purpose of this part of our study was to achieve a high selectivity of the catalytic membrane module with respect to the first two reactions.

Figure 7 illustrates the changes in the porosity of the cermet membrane upon the formation, in its microchannels, of the catalytic system $Cr_2O_3 \cdot Al_2O_3 \cdot ZnO$ to be tested in the above reactions. As is clear from Fig. 7, the strongest peak in the pore-size distribution of the original membrane is that at 90 nm. This result checks well with the certificate of the membrane [10]. For the membrane containing the catalytic system, this macropore peak is shifted to 73 nm and a peak at 2.4 nm is observed in the micropore region. Most likely, the microporous structure is due to the metal oxide film inside the membrane channels.

At high values of methanol conversion on the tubular ceramic membrane, which has a large catalytic surface, the main methanol conversion pathway is towards

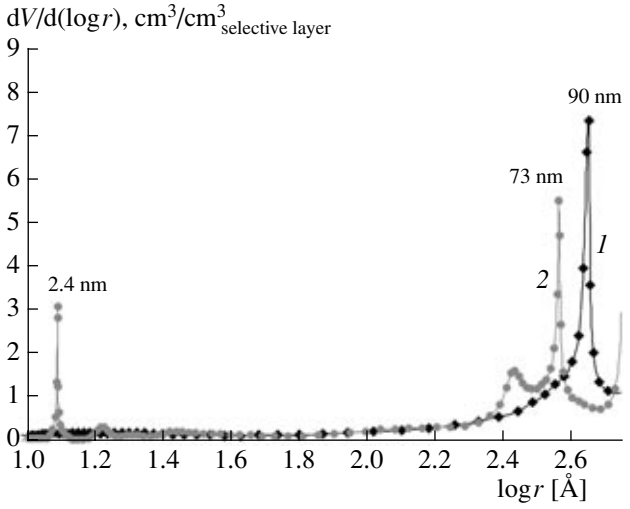

Fig. 7. Pore-size (r) distribution for the flexible membrane: (*1*) original membrane and (*2*) the same membrane after the formation of the catalytic system.

synthesis gas (Table 3). With cermet disc membrane modules, which have a small surface area, methanol conversion is no higher than 5% at 300°C and is dominated by the dehydrogenation reaction.

It is believed that establishing conditions favoring the selective transport of gaseous products of this reaction will raise the hydrogen yield. For this purpose, we developed a hybrid catalytic membrane module: an oxide catalytic system was formed in the channels of the cermet membrane, and the geometrical surface of the membrane was coated with a mesoporous metal oxide membrane layer. Earlier, we developed a method for the synthesis of fine $P_{0.03}Ti_{0.97}O$ powder with a narrow pore-size distribution around $\langle d \rangle \sim 2$ nm and studied the structure of this oxide [18, 33]. This material was obtained by spin coating as a thin layer on the geometrical surface of the cermet membrane. Figure 8 presents gas permeability data for a membrane coated with a thin phosphorus–titanium oxide layer with a uniform pore size. In the unmodified membrane, whose catalyst content is up to 0.7 g/cm^3, the transmembrane flow is viscous. After coating the surface of this membrane

Table 3. Data characterizing (1) methanol conversion into synthesis gas and (2) methanol dehydrogenation (T = 300°C, $Cr_2O_3 \cdot Al_2O_3 \cdot ZnO$ catalyst)

Catalytic membrane module	V_{MeOH}, h^{-1}	S, %		Output, mmol g^{-1} h^{-1}
		1	2	
Tube	24.18	90	10	30.3
Uncoated disc	120	18	82	15.3
Disc coated with $P_{0.03}Ti_{0.97}O_2$	120	8	92	86.5

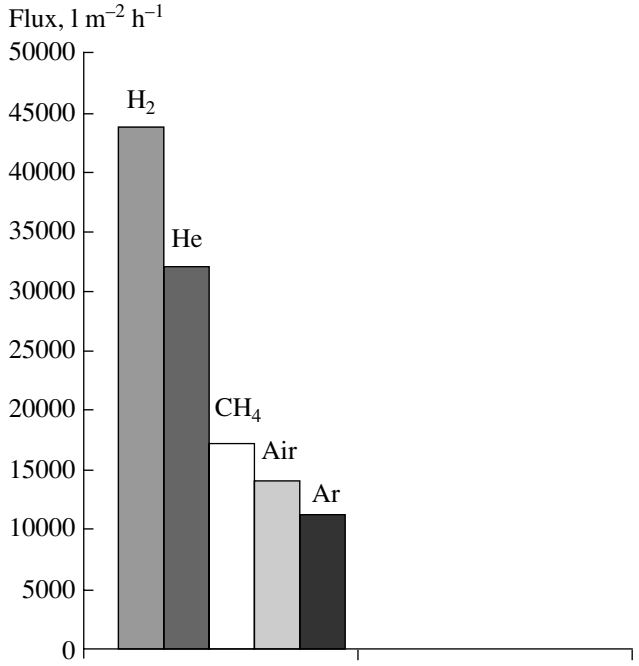

Fig. 8. Gas permeability diagram for the membrane modified with a phosphorus–titanium oxide film.

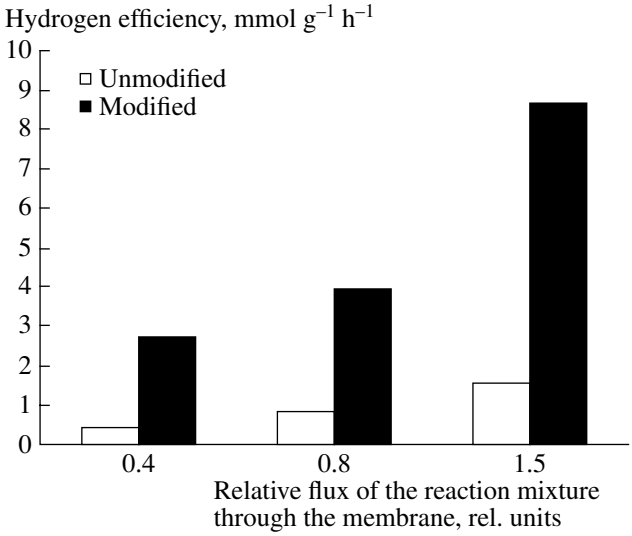

Fig. 9. H_2 efficiency diagram for methanol dehydrogenation in a catalytic membrane module before and after the modification of the membrane with a phosphorus–titanium oxide film.

with a thin mesoporous layer, the gas permeates through the membrane in the Knudsen flow regime, and the transmembrane transport is selective (Fig. 8).

In Fig. 9, we present a hydrogen efficiency diagram for methanol dehydrogenation (5% conversion) at 300°C in a catalytic membrane module before and after the membrane surface is coated with a thin mesoporous layer. Clearly, the hydrogen efficiency of methanol conversion is half an order of magnitude higher for the membrane modified with a thin mesoporous layer. Coating the membrane surface with mesoporous oxide raises the nonoxidative MeOH dehydrogenation selectivity from ~80 to 90%.

Further nanoreactor design studies were aimed at the production of zeolite coatings on the geometrical surface of the membrane. In this case, the pore size could be decreased to 10 Å and this would further enhance the selectivity of the transport of gaseous products. It was demonstrated in earlier studies [19, 34] that zeolite microcrystals form microblocks on the membrane surface and that the full coverage of the surface can be achieved only by successively producing several layers of such microblocks. Uniformly oriented zeolite blocks can be obtained only on a specially prepared surface. We failed to produce a zeolite coating directly on the cermet surface. It was necessary to cover the cermet surface with a uniformizing buffer film. We used a mesoporous layer of phosphorus–titanium oxide as the buffer. Figure 10a shows a scanning electron micrograph of uniformly oriented zeolite blocks covering a rather large area of the phosphorus–titanium oxide buffer film. Note that crystallites can be orientated only on a highly uniform film. In the specimen examined, the orientation of crystallites is disordered near microcracks in the buffer film. It was found that these microcracks had formed at the heat treatment stage of the preparation of the buffer oxide film from organic mother solutions of metal complex precursors. These defects are hidden by overlying thin oxide films produced in subsequent deposition runs. This is indirectly indicated by gas permeability data. However, these defects cannot be completely healed, giving rise to nonuniformities in the film. Unfortunately, this affects the orientation of zeolite crystallite blocks. The micrograph shown in Fig. 10b is a top view of such a system. At microcrack sites, the orientation of blocks is changed to form elongated one-dimansional strings.

The conditions favoring the formation of thin buffer films for surface uniformization will be the subject of forthcoming studies.

The following conclusions can be drawn from the results of the initial stage of our nanoreactor design study.

The use of sol–gel processing as a design means enables one to carry out controlled syntheses of mixed oxide films modifying the mechanical, catalytic, and gas-separation properties of ceramic membranes.

A variety of reactions involving C_1 compounds can be intensified in membrane channels modified with finely dispersed metal oxides. It is significant that the development of a catalytic reaction is observed when the gas flow is still viscous. This effect points to transient diffusion, a poorly understood flow regime char-

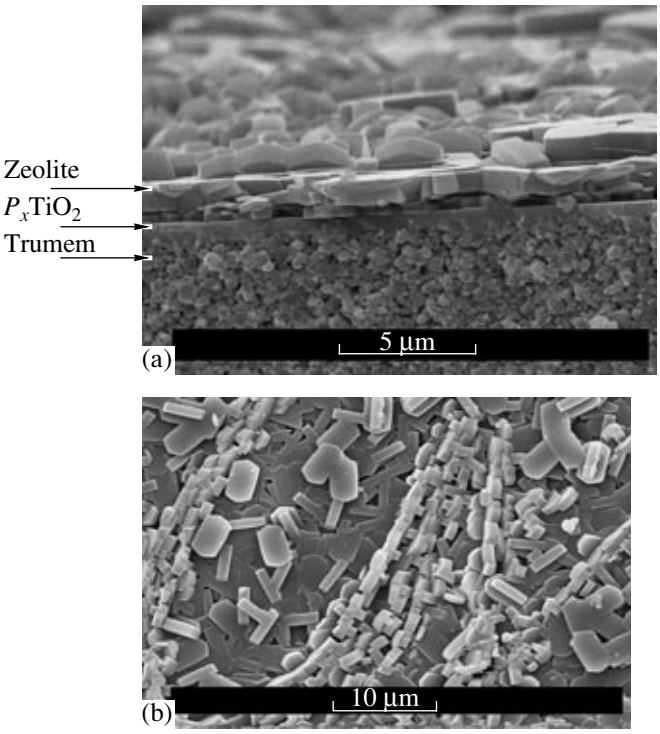

Fig. 10. Morphology of the hybrid membrane system containing a zeolite film: (a) SEM image and (b) top view.

acterized by an increased contribution from surface flows. It is likely that the compensation effect observed in CO oxidation is accompanied by an increase in the contribution from surface diffusion.

Methods have been suggested for the formation of mesoporous–microporous multilayered membrane systems ensuring the selective transport of gaseous reaction products. It has been demonstrated by the example of nonoxidative methanol dehydrogenation that reaction selectivity can be enhanced by using a catalytic membrane reactor. From the structural standpoint, this type of reactor is an ensemble of catalytic nanochannels (nanoreactors).

ACKNOWLEDGMENTS

This work was supported by the Russian Foundation for Basic Research (project no. 02-03-33053) and the NWO Foundation (project no. 047.015.009).

REFERENCES

1. Ditmeyer, R., Svajda, K., and Reif, M., *Top. Catal.*, 2004, vol. 29, nos. 1–2, p. 3.
2. Miachon, S. and Dalmon, J.A., *Top. Catal.*, 2004, vol. 29, nos. 1–2, p. 59.
3. Wang, H.H., Cong, Y., and Yang, W.S., *Catal. Today*, 2003, vol. 82, nos. 1–4, p. 157.
4. Chen, C., Feng, Sh., Ran, S., Zhu, D., Liu, W., and Bouwmeester, J.M., *Angew. Chem., Int. Ed. Engl.*, 2003, vol. 42, p. 5196.
5. Balachandran, U., Dusek, J.T., Mieville, R.L., Poeppel, R.B., Kleefisch, M.S., Pei, S., Kobulinski, T.P., Udovich, C.A., and Bose, A.C., *Appl. Catal., A*, 1995, vol. 133, p. 19.
6. Hwang, S.T. and Kammermeyer, K., *Membranes in Separations*, New York: Wiley, 1975.
7. Vilani, S. and Kikoin, I.K., *Obogashchenie urana* (Uranium Enrichment), Moscow: Energoatomizdat, 1983, p. 51.
8. Turova, N.Ya., Turevskaya, E.P., and Yanovskaya, M.I., *The Chemistry of Metal Alkoxides*, Amsterdam: Kluwer, 2001.
9. Trusova, E.A., Tsodikov, M.V., Slivinskii, E.V., Hernandez, G.G., Bukhtenko, O.V., Gdanova, T.N., Kochubey, D.I., and Navio, J.A., *Mendeleev Commun.*, 1998, vol. 3, p. 102.
10. Trusov, L.I., *J. Membr. Technol.*, 2000, no. 128, p. 10.
11. RF Patent 2175904, 2002.
12. Tsodikov, M.V., Laguntsov, N.I., Magsumov, M.I., Spiridonov, P.V., Bukhtenko, O.V., Zhdanova, T.N., and Teplyakov, V.V., *Izv. Akad. Nauk, Ser. Khim.*, 2004, no. 9, p. 6.
13. Tsodikov, M.V., Teplyakov, V.V., Spiridonov, P.V., Magsumov, M.I., Kapteijn, F., Gora, L., and Moiseev, I.I., *2nd Int. Conf. on Highly-Organized Catalytic Systems*, Moscow, 2004, p. 46.
14. Tsukama, K., Kend, V., and Shimada, M., *J. Am. Ceram. Soc.*, 1985, vol. 68, p. 4.
15. Ellert, O.G., Petrunnenko, I.A., Tsodikov, M.V., Bukhtenko, O.V., Kochubey, D.I., Maksimov, Yu.V., and Domingez-Rodrigez, A., *J. Mater. Chem.*, 1996, vol. 6, no. 2, p. 207.
16. Ellert, O.G., Petrunenko, I.A., Tsodikov, M.V., Bukhtenko, O.V., Kochubey, D.I., Maksimov, Yu.V., Dominges-Rodrigez, A., Cumbrera, E.L., and Navio, J.A., *J. Sol–Gel Sci. Technol.*, 1997, vol. 8, p. 213.
17. Sakulin, V.V., Aronovich, R.A., Slivinskii, E.V., Egorov, E.F., Moskovskii, Yu.D., Patrusheva, V.A., Mazaeva, V.A., and Bol'shakov, V.A., *Osnovn. Org. Sint. Neftekhim.*, 1993, vol. 28, p. 7.
18. Tsodikov, M.V., Bukhtenko, O.V., Slivinskii, E.V., Slastikhina, L.N., Voloshchuk, A.M., Kriventsov, N.V., and Kitaev, L.E., *Izv. Akad. Nauk, Ser. Khim.*, 2000, no. 11, p. 52.
19. Annemieke, W.C., van den Berg, Gora, L., and Jansen, J.C., and Maschmeyer, Th., *Microporous Mesoporous Mater.*, 2003, vol. 66, p. 303.
20. Shkol'nikov, E.I. and Volkov, V.V., *Dokl. Akad. Nauk*, 2001, vol. 378, no. 4, p. 507.
21. Pajares, A., Guiberteau, F., Westmacott, K.H., and Domingez-Rodrigez, A., *J. Mater. Sci.*, 1993, vol. 28 P, p. 6709.
22. Sanchoz-Bajo, F., Cumbrera, F.L., Guibertear, F., Domingez-Rodrigez, A., and Tsodikov, M.V., *Mater. Lett.*, 1998, vol. 33, p. 283.
23. Schmid, R., Ahamdan, H., and Mosset, A., *Inorg. Chim. Acta*, 1991, vol. 190, p. 237.

24. Tsodikov, M.V., Bukhtenko, O.V., Ellert, O.G., Shcherbakov, V.M., and Kochubey, D.I., *J. Mater. Sci.*, 1995, vol. 30, p. 1087.
25. Ernandes, G.F., *Cand. Sci. (Chem.) Dissertation*, Moscow: Topchiev Institute of Petrochemical Synthesis, 1999.
26. Roginskii, S.Z., *Probl. Kinet. Katal.*, 1944, vol. 6, p. 9.
27. Roginskii, S.Z., *Geterogennyi kataliz v khimicheskoi promyshlennosti* (Heterogeneous Catalysis in the Chemical Industry), Moscow: Goskhimizdat, 1955.
28. Poltorak, O.M., *Lektsii po teorii kataliza* (Lectures on Catalysis Theory), Moscow: Mosk. Gos. Univ., 1968.
29. Levich, V.G., *Kurs teoreticheskoi fiziki* (Theoretical Physics), Moscow: Nauka, 1960.
30. Wert, Ch.A. and Thomson, R.M., *Physics of Solids*, New York: McGraw-Hill, 1964, p. 563.
31. Dedov, A.G., Loktev, A.S., Men'shchikov, V.A., Filimonov, I.N., Parkhomenko, K.V., and Moiseev, I.I., *Dokl. Akad. Nauk*, 2001, vol. 380, no. 6, p. 791.
32. Stull, D.R., Wesrtum, E.F., and Sinke, G.C., in *The Chemical Thermodynamics of Organic Compounds*, New York: Wiley, 1969.
33. Kozlovskii, R.A., Yushchenko, V.V., Kitaev, L.E., and Tsodikov, M.V., *Izv. Akad. Nauk, Ser. Khim.*, 2002, no. 6, p. 887.
34. Coronas, J. and Santamaria J, *Top. Catal.*, 2004, vol. 29, nos. 1–2, p. 3.